Machine learning study of fission barriers in superheavy nuclei

Jiaxing Li[1] and Hongfei Zhang[1,2,*]

[1]*School of Physics, Xi'an Jiaotong University, 710049 Xi'an, People's Republic of China*

[2]*School of Nuclear Science and Technology, Lanzhou University, 730000 Lanzhou, People's Republic of China*

(Received 12 April 2024; revised 18 July 2024; accepted 22 August 2024; published 11 September 2024)

The synthesis of superheavy elements represents the forefront of exploring the properties of unknown nuclear matter. Theoretically, significant uncertainties in predicting the fission barriers of superheavy nuclei make accurate calculations of the survival probabilities of compound nuclei extremely challenging. This study utilizes a machine learning methodology to predict the fission barriers of nuclides with $93 < Z \leqslant 120$ and $135 < N \leqslant 184$. We have estimated the fission barriers for a total of 660 nuclides, and leveraged these fission barriers to calculate the crucial survival probabilities in the synthesis of superheavy elements. Based on this, we calculated the reaction cross sections for the $^{48}\mathrm{Ca} + ^{243}\mathrm{Am}$ reaction within the framework of the dinuclear system model, and compared the results with experimental data measured using the new gas-filled separator DGFRS-2. The calculations successfully reproduced the experimental data within an acceptable range of error. Additionally, we explored the optimal synthesis conditions for synthesizing the new elements $Z = 119$ and $Z = 120$, including projectile-target combinations, incident energies, and maximum reaction cross sections.

DOI: 10.1103/PhysRevC.110.034608

I. INTRODUCTION

The synthesis of new elements is a forefront topic in nuclear physics [1–3]. By successfully synthesizing element 118, the expansion of the periodic table has not only deepened our understanding of nuclear structure but also advanced progress in physics, chemistry, and interdisciplinary fields [4–7]. However, the synthesis of the new elements 119 and 120 poses significant scientific and technical challenges [2,8,9]. The most important challenge in synthesizing new elements is to choose the optimal projectile-target combination and the optimal incident energy to obtain the maximum reaction cross section [10–12].

The key to successfully synthesizing new elements is their stability, which depends on their ability to resist fission [13–16]. Thus, accurately determining the fission barrier is essential for predicting the synthesis of new elements [17–19]. However, the scarcity of experimental data, coupled with discrepancies among theoretical models, introduces substantial uncertainties into the current predictions of fission barriers for superheavy elements [20]. In Ref. [21], experimental data on fission barriers are available only up to atomic number $Z = 96$, with no data available for superheavy nuclei. The fission barriers used in the calculation of survival probabilities for superheavy nuclei are usually estimated using various theoretical models. Common models for estimating the fission barriers include the finite range liquid drop model (FRLDM) [22], the extended Thomas-Fermi plus Strutinsky integral (ETFSI) based on the Skyrme SkSC4 functional [23,24], the Lublin-Strasbourg drop (LSD) approach [25,26], and the heavy nucleus (HN) model [17]. These models generally show a deviation within 2 MeV from the experimental values for the actinide fission barriers. In the superheavy nuclear region where experimental data are lacking, the predicted fission barriers differ significantly. The highest difference in the fission barriers for the isotopic chains of $Z = 112$–120 reaches up to 6 MeV [27]. Such a large margin of error is unacceptable for estimating survival probabilities.

In recent years, machine learning have been widely applied in the field of nuclear physics, for tasks such as calculating alpha decay half-lives [28], estimating beta decay energies [29], and predicting nuclear masses [30–32]. We also noticed some other works, such as a machine learning framework successfully encoding several correlated aspects of nuclear deformation [33], and neural networks being able to emulate potential energy and collective inertia well [34]. These are sufficient to illustrate the important role of machine learning in nuclear physics. For the study of superheavy nuclear fission processes, Ref. [35] shows that the spontaneous fission half-lives predicted by the FRLDM are usually longer than the experimental values. However, the overall trend of these predictions aligns well with the experimental data. This suggests that the FRLDM captures most of the essential physics but misses some aspects, resulting in fission barrier values that are typically higher than those observed experimentally. In this paper, we address this discrepancy by first pretraining an artificial neural network (ANN) on the fission barrier data provided by the FRLDM. This pretraining helps the ANN learn the general physical characteristics. We then apply transfer learning, using a limited set of experimental data to fine tune the model.

Our goal is to reasonably predict the fission barriers in the region of superheavy nuclei, which is a crucial step in

*Contact author: zhanghongfei@lzu.edu.cn

calculating the survival probability. Subsequently, based on the dinuclear system model, the optimal projectile-target combination, optimal incident energy, and maximum reaction cross section are explored for the synthesis of new elements. In Sec. II, we introduce the theoretical framework. In Sec. III, we analyze and discuss the results. In Sec. IV, we summarize our work.

II. THEORETICAL FRAMEWORK

A. Neural network details

The ANN architecture includes an input layer, two hidden layers, and an output layer. The input layer accepts two main features: Z and N, representing the number of protons and neutrons, respectively. These inputs are processed through two consecutive hidden layers, each containing 64 neurons. The use of the ReLU (rectified linear unit) activation function in these hidden layers introduces nonlinear functionality. The output layer has a separate neuron for predicting the fission barrier. The ANN is trained using two datasets: theoretical data and experimental data. First, the model is pretrained on theoretical data. Then, it uses transfer learning techniques to retrain on experimental data for fine tuning the model. The transfer learning method implemented in this study retrains the last layer of the network with experimental data. Simply put, the ANN first learns general physical features from theoretical data and then trains on experimental data to find the missing physics. During the training process, the mean squared error (MSE) loss function is used, which is expressed as

$$\mathrm{MSE} = \frac{1}{N}\sum_{i=1}^{N}(B_i - B_{\mathrm{ANN},i})^2, \tag{1}$$

where N represents the total number of data points, B_i the desired output, and $B_{\mathrm{ANN},i}$ the output from the ANN. The model uses the Adam optimizer with an initial learning rate of 0.001. Training spans 5000 epochs, with batch processing and early stopping based on validation loss to avoid overfitting. Regular evaluations on the validation set help monitor performance and adjust training as needed.

B. Calculating production cross section details

The production cross section, denoted as σ, is expressed as

$$\sigma = \sigma_{\mathrm{cap}} \times P_{\mathrm{cn}} \times W_{\mathrm{sur}}, \tag{2}$$

here, σ_{cap} represents the capture cross section, which can be calculated using the empirical coupled channel model [36]. Detailed descriptions of the calculations for the capture cross section can be obtained from Ref. [18]. P_{cn} is the probability of the evolution of the system from the contact configuration to the formation of the compound nucleus. The fusion probability of the dinuclear system is given by

$$P_{\mathrm{cn}}(E_{\mathrm{c.m.}}, J) = \sum_{Z_1=1}^{Z_{\mathrm{BG}}}\sum_{N_1=1}^{N_{\mathrm{BG}}} P(Z_1, N_1, E_1, \tau_{\mathrm{int}}), \tag{3}$$

here, the time evolution of the distribution probability function $P(Z_1, N_1, E_1, t)$ can be obtained by solving the master equation in the corresponding potential energy surface [37]. The N_{BG} and Z_{BG} are the neutron number and proton number at the Businaro-Gallone point respectively. The fission barriers are crucial for estimating the survival probabilities of superheavy nuclei. During the deexcitation of an excited compound nucleus, there is competition between neutron evaporation and fission [38,39]. The survival probability of emitting xn neutrons can be written as [40]

$$W_{\mathrm{sur}}(E^*_{\mathrm{CN}}, x, J) = P(E^*_{\mathrm{CN}}, x, J)\prod_{i=1}^{x}\left[\frac{\Gamma_n}{\Gamma_n + \Gamma_f}\right]_i, \tag{4}$$

in the formula, E^*_{CN} represents the excitation energy of the compound nuclei. $P(E^*_{\mathrm{CN}}, x, J)$ is the realization probability of emitting x neutrons, which is addressed in detail in Ref. [16]. The neutron evaporation width Γ_n and the fission width Γ_f are calculated using a statistical model [18].

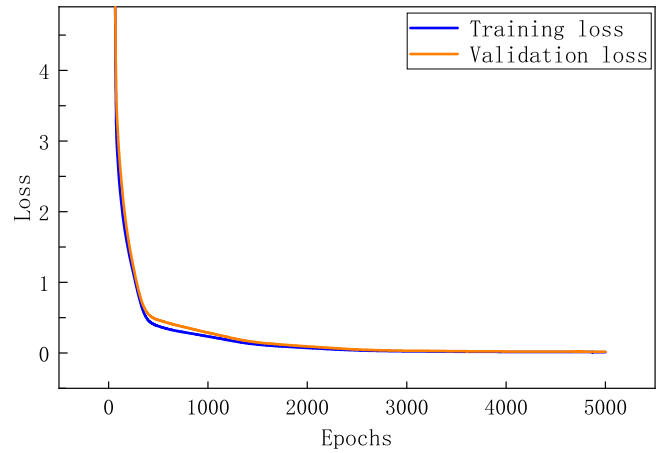

FIG. 1. Training and validation loss curves.

III. RESULTS AND DISCUSSION

A. ANN fission barrier estimations

In the pretraining phase, the ANN consists of three fully connected layers: an input layer with two feature values, two hidden layers with 64 neurons, and an output layer representing the fission barriers of the considered nuclei. The data for the fission barriers are sourced from the FRLDM [22], focusing on nuclear ranges with proton numbers $93 < Z \leqslant 120$, neutron numbers $135 < N \leqslant 184$, and mass numbers $A > 239$, encompassing a total of 660 datasets. We divided the 660 datasets into a training set and a validation set with a ratio of 6:4. The loss curves for both the training set and validation set are illustrated in Fig. 1. The blue line represents the loss on the training set, indicating the model's performance in learning from the training data. The orange line represents the loss on the validation set, reflecting how well the model generalizes to unseen data. The consistent decrease in loss over epochs suggests effective learning, and the close tracking of both lines indicates a balanced fit without evident signs of overfitting or underfitting.

In the transfer learning phase, the weights of the model's input layer and hidden layers are frozen. This means that

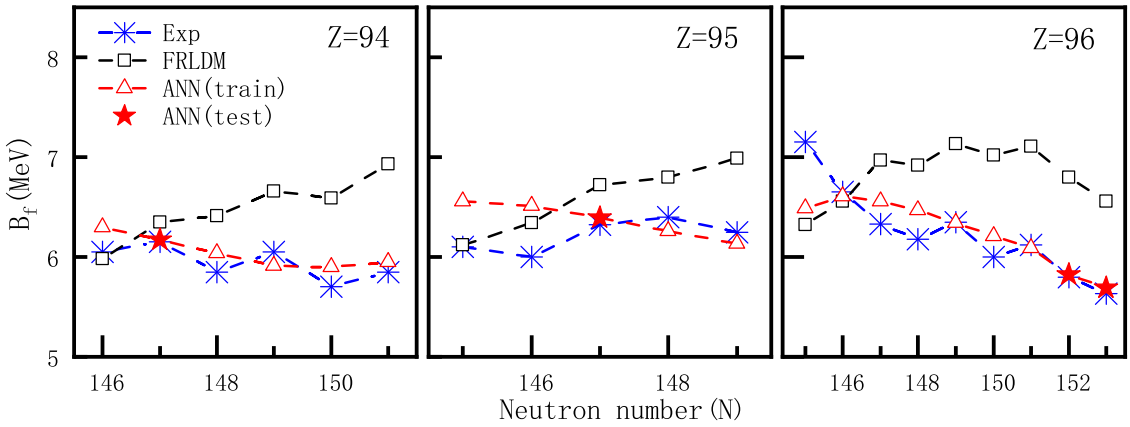

FIG. 2. Comparison of experimental and theoretical estimations of fission barriers B_f: blue stars represent experimental results (from Ref. [21]), black squares denote FRLDM results (from Ref. [22]), red triangles indicate results from our ANN for 16 training and validation sets, and solid red stars show our ANN results for four test sets.

the weights of these layers do not change during the transfer learning process. We only retrain the output layer, and the weights of this layer will be updated and retrained based on the experimental data set, thereby fine tuning the pretrained network. In this study, the experimental data are obtained from Ref. [21], focusing on nuclear ranges with proton numbers $93 < Z \leqslant 120$, neutron numbers $135 < N \leqslant 184$, and mass numbers $A > 239$, comprising a total of 20 data points. This experimental dataset is initially split such that 80% is used for both training and validation purposes, while the remaining 20% is reserved as the test set, crucial for evaluating the model's performance on unseen data. Further, the 80% portion allocated for training and validation is subdivided, with 60% used as the training set and the remaining 40% serving as the validation set. Figure 2 presents the estimated values from our ANN (a total of 20 data points, with 16 from the training and validation sets, and 4 from the test set), and compares them with the experimental values and the estimated values from the FRLDM. One can observe that the results estimated by our ANN are very close to the experimental values, with a maximum deviation not exceeding 0.7 MeV. Furthermore, the FRLDM estimated results exhibit an MSE of 0.491 MeV for all 20 data points, while the ANN estimated results have an MSE of 0.0651 MeV for the same 20 data points. Notably, the ANN estimated results show an MSE of only 0.00233 MeV when compared to the four test data points. These findings suggest that the ANN approach is suitable for estimating fission barriers.

We also used ANN to estimate the fission barriers of superheavy nuclei, which are far from the actinide nuclei with experimental data used in transfer learning, to understand the predictive capability of the ANN method. In Table I, we compare several theoretical estimations with experimental data. Notably, the experimental data in Ref. [42] only provides lower limit values. As we observed, both FRLDM [22] and SHF [41] significantly overestimate the fission barriers. For nuclide ^{292}114, FRLDM predicts a value of 9.98 MeV, which is about 3 MeV higher than the experimental value. For nuclide ^{294}116, SHF predicts 9.59 MeV, also considerably higher than the experimental data. Meanwhile, HN [17] and ETFSI [24] estimates for the fission barriers of nuclides ^{284}112 and ^{286}112 are lower than the lower limits of the experimental values. Our ANN results are slightly higher than the experimental values, ranging from 0.7 to 1.7 MeV above, but, considering that the experimental data represents lower limits, the fission barriers predicted by the ANN in the superheavy region are relatively reasonable, further demonstrating the effectiveness of the ANN approach.

In Fig. 3, we show the contour map of estimated fission barriers by FRLDM and ANN. The figure contains the fission barriers for superheavy nuclei in the range of proton numbers $93 < Z \leqslant 120$, neutron numbers $135 < N \leqslant 184$, and mass numbers $A > 239$ (totaling 660 data points). It can be seen that for the entire range of nuclei considered, the fission barriers estimated by FRLDM are all below about 10 MeV, and those by ANN are all below about 8 MeV. The range with higher fission barriers for both occurs approximately within

TABLE I. Comparison of fission barriers (in MeV) of superheavy nuclei with other theoretical evaluations: SHF [41], HN [17], ETFSI [24], FRLDM [22], ANN (present paper), and experimental data (the lower limits) taken from Ref. [42].

Nucleus	SHF	HN	ETFSI	FRLDM	ANN	Exp
^{283}112			2.20	6.99	6.21	5.50
^{284}112	6.06	4.29	2.20	7.41	6.41	5.50
^{285}112			2.70	8.00	6.61	5.50
^{286}112	6.91	5.01	3.60	8.24	6.80	5.50
^{288}114	8.12	5.53	6.10	9.18	7.75	6.70
^{289}114			6.70	9.61	7.92	6.70
^{290}114	8.52	5.83	6.60	9.89	7.91	6.70
^{291}114			7.30	9.97	7.89	6.70
^{292}114		6.34	7.20	9.98	7.87	6.70
^{292}116	9.35	6.22	6.50	9.26	8.01	6.40
^{293}116			7.00	9.35	8.03	6.40
^{294}116	9.59	6.28	7.20	9.46	8.06	6.40
^{295}116			7.70	9.49	8.08	6.40
^{296}116		6.07	7.60	9.10	7.90	6.40

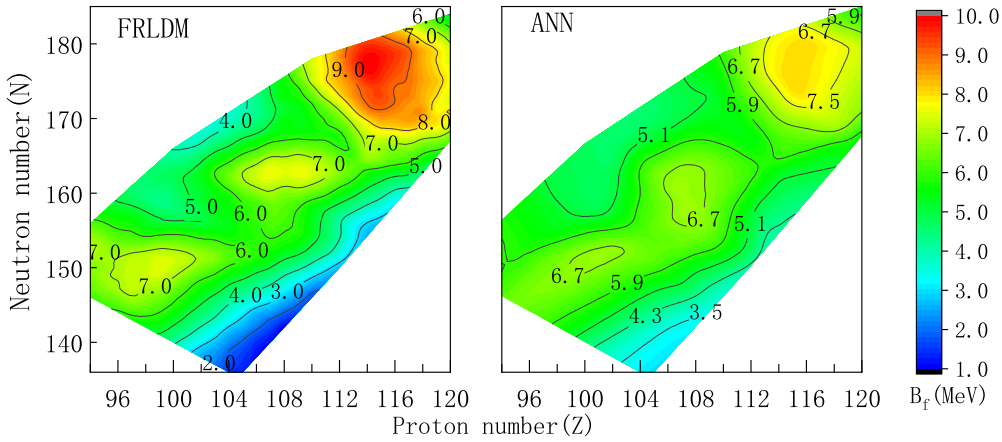

FIG. 3. Contour map of estimated fission barriers B_f for superheavy nuclei.

$114 \leqslant Z \leqslant 116$ and $174 \leqslant N \leqslant 180$. Within this range, the fission barriers estimated by ANN are overall 1–2 MeV lower than those estimated by FRLDM.

B. Production cross sections of superheavy nuclei

The fission barriers are crucial for estimating the survival probabilities of superheavy nuclei. During the deexcitation of an excited compound nucleus, there is competition between neutron evaporation and fission [38,39]. In Fig. 4, we present the survival probabilities calculated using different fission barriers. The fission barriers estimated by FRLDM are typically higher, leading to higher survival probabilities. It is clear that varying fission barriers used in calculations cause significant differences in survival probabilities, sometimes even by an order of magnitude. Hence, selecting relatively accurate fission barriers is crucial for estimating survival probabilities and cross sections in heavy-ion fusion reactions.

Currently, there is relatively more experimental data on the reaction cross section for $^{48}\mathrm{Ca} + ^{243}\mathrm{Am}$ [6,43–45], including the latest results generated at the new gas-filled separator DGFRS-2 of the superheavy element factory at JINR [44,45]. Based on the obtained survival probability, we calculated the cross section for the reaction within the framework of the dinuclear system model. In Fig. 5, we present the cross sections for the reaction $^{48}\mathrm{Ca} + ^{243}\mathrm{Am}$, and compare them with experimental data. According to Ref. [44],

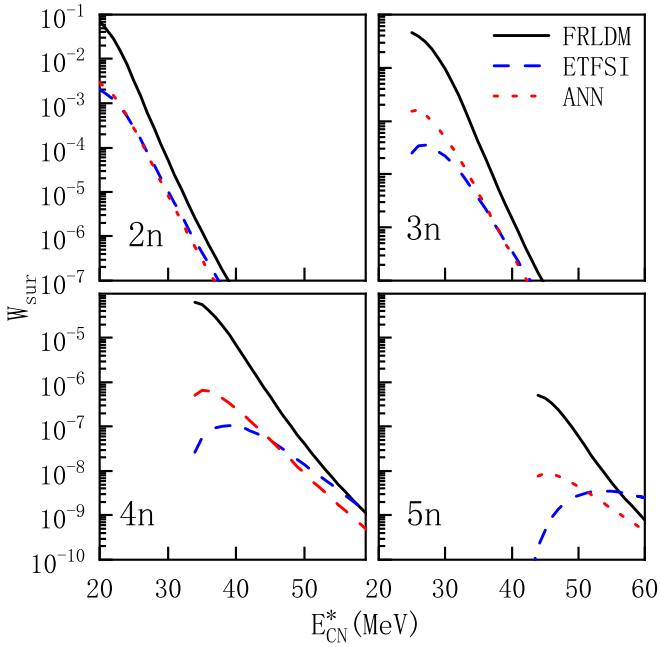

FIG. 4. The survival probabilities for the $2n$, $3n$, $4n$, and $5n$ evaporation channels in the $^{48}\mathrm{Ca} + ^{243}\mathrm{Am} \rightarrow ^{291-xn}115 + xn$ reaction.

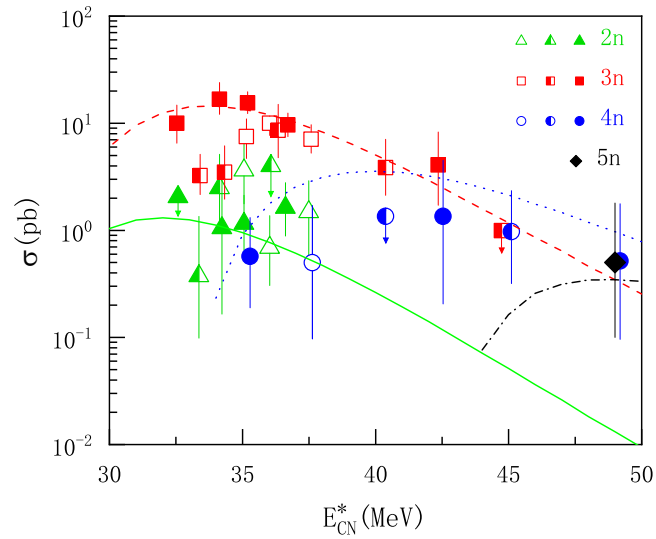

FIG. 5. Production cross sections for the $2n$, $3n$, $4n$, and $5n$ evaporation channels in the $^{48}\mathrm{Ca} + ^{243}\mathrm{Am} \rightarrow ^{291-xn}115 + xn$ reaction. Vertical error bars indicate total uncertainties. Symbols with arrows denote upper cross section limits. Data are represented by open symbols (from Ref. [43]), half-closed symbols (from Ref. [6]), and closed symbols (representing the latest results obtained with the DGFRS-2, from Refs. [44,45]). The lines are the result of our calculation.

TABLE II. Estimated fission barriers for isotopic chains of $Z = 119$ and $Z = 120$ by our ANN.

Nucleus	B_f (MeV)	Nucleus	B_f (MeV)
$^{292}119$	7.23	$^{297}120$	7.30
$^{293}119$	7.31	$^{298}120$	7.37
$^{294}119$	7.39	$^{299}120$	7.29
$^{295}119$	7.47	$^{300}120$	6.93
$^{296}119$	7.52	$^{301}120$	6.57
$^{297}119$	7.54	$^{302}120$	6.21

the cross section for the $3n$ evaporation channel in the reaction $^{48}\mathrm{Ca} + ^{243}\mathrm{Am}$, measured through DGFRS-2, is $17.1^{+6.3}_{-4.7}$ pb. This is about twice the value measured by DGFRS in Ref. [6], and it is the largest value for the known superheavy nuclei at the island of stability. In the $3n$ evaporation channel, our calculation resulted in a maximum cross section of 14.45 pb, which astonishingly corresponds with the results produced at DGFRS-2. In these experiments, products of the $4n$ evaporation channel were observed within an excitation energy range of 35–49 MeV, with the maximum measured cross section at about 42 MeV being $1.4^{+3.2}_{-1.2}$ pb. In the $4n$ channel, at an excitation energy of 42 MeV, our calculated result is 3.23 pb, again consistent with experimental values. Reference [45] first reported results for the $5n$ evaporation channel of this reaction, with a cross section of $0.5^{+1.3}_{-0.4}$ pb at $E^*_{\mathrm{CN}} = 49$ MeV. Our calculations show a cross section of 0.35 pb at $E^*_{\mathrm{CN}} = 49$ MeV, fitting well within the error margin of the experimental data. Within the framework of the dinuclear system model, the cross sections calculated using the fission barriers estimated by our ANN have accurately reproduced the latest results measured at DGFRS-2, which also indirectly demonstrates the effectiveness of our ANN. To further study the synthesis and properties of new elements $Z = 119$ and $Z = 120$, we have provided in Table II the fission barriers of isotopic chains of $Z = 119$ and $Z = 120$ as estimated by our ANN. It can be seen that the fission barriers of these nuclei are all about 6 MeV or higher, suggesting that compared to previously synthesized superheavy nuclei, the probability of survival does not decrease rapidly. In the synthesis of superheavy elements, ^{48}Ca has traditionally been the projectile of choice [46], extending the periodic table to element 118. For the synthesis of new elements $Z = 119$ and $Z = 120$, due to the lack of suitable target nuclei, ^{54}Cr has been selected as the projectile. In Fig. 6, we present the production cross sections for the $2n$, $3n$, $4n$, and $5n$ evaporation channels in the reactions using ^{54}Cr to synthesize new elements $Z = 119$ and $Z = 120$. It is observed that for the synthesis of $Z = 119$, the optimal incident energy is 241.65 MeV, with a maximum production cross section of 0.005 68 pb. For the synthesis of $Z = 120$, the optimal incident energy is identified as 251.85 MeV, with a maximum production cross section of 0.00019 pb.

IV. SUMMARY

This study presents an effective ANN model that can quickly estimate fission barriers affecting the survival probability of superheavy nuclei. The model provides 660 fission barrier estimates for nuclei ranging from $Z = 93$ to $Z = 120$ and $N = 135$ to $N = 184$. While we cannot determine the exact accuracy of these estimates, they appear reasonable based on current experimental data. Additionally, this study highlights the importance of fission barrier in calculating the survival probability of heavy-ion fusion reactions. Leveraging these fission barriers, we reconstructed the experimental reaction cross section of $^{48}\mathrm{Ca} + ^{243}\mathrm{Am}$ within the framework of the dinuclear system model and explored the optimal incident energy and maximum reaction cross section for synthesizing new elements. We hope our research provides insights for the study of superheavy nuclei reactions and structures.

ACKNOWLEDGMENT

This work is supported by National Natural Science Foundation of China (Grants No. 12175170 and No. 11675066).

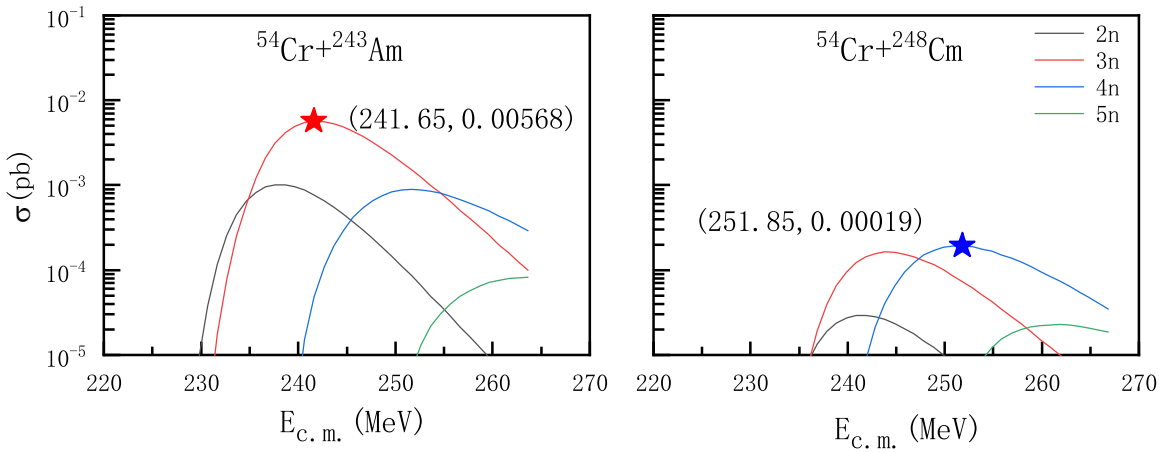

FIG. 6. Production cross sections for $2n$, $3n$, $4n$, and $5n$ evaporation channels in the reactions producing new elements $Z = 119$ and $Z = 120$.

[1] G. Herrmann, Nature (London) **280**, 543 (1979).
[2] O. R. Smits, C. E. Düllmann, P. Indelicato, W. Nazarewicz, and P. Schwerdtfeger, Nat. Rev. Phys. **6**, 86 (2024).
[3] J. C. Pei, W. Nazarewicz, J. A. Sheikh, and A. K. Kerman, Phys. Rev. Lett. **102**, 192501 (2009).
[4] W. Nazarewicz, Nat. Phys. **14**, 537 (2018).
[5] Y. T. Oganessian, V. K. Utyonkov, Y. V. Lobanov, F. S. Abdullin, A. N. Polyakov, R. N. Sagaidak, I. V. Shirokovsky, Y. S. Tsyganov, A. A. Voinov, G. G. Gulbekian *et al.*, Phys. Rev. C **74**, 044602 (2006).
[6] Y. T. Oganessian, F. S. Abdullin, S. N. Dmitriev, J. M. Gostic, J. H. Hamilton, R. A. Henderson, M. G. Itkis, K. J. Moody, A. N. Polyakov, A. V. Ramayya *et al.*, Phys. Rev. C **87**, 014302 (2013).
[7] Y. T. Oganessian, V. K. Utyonkov, Y. V. Lobanov, F. S. Abdullin, A. N. Polyakov, I. V. Shirokovsky, Y. S. Tsyganov, G. G. Gulbekian, S. L. Bogomolov, B. N. Gikal *et al.*, Phys. Rev. C **69**, 054607 (2004).
[8] S. Hofmann, S. Heinz, R. Mann, J. Maurer, G. Münzenberg, S. Antalic, W. Barth, H. Burkhard, L. Dahl, K. Eberhardt *et al.*, Eur. Phys. J. A **52**, 180 (2016).
[9] C. E. Düllmann, EPJ Web. Conf. **131**, 08004 (2016).
[10] G. G. Adamian, N. V. Antonenko, H. Lenske, and L. A. Malov, Phys. Rev. C **101**, 034301 (2020).
[11] A. Nasirov and B. Kayumov, Phys. Rev. C **109**, 024613 (2024).
[12] F. Niu, P.-H. Chen, and Z.-Q. Feng, Nucl. Sci. Tech. **32**, 103 (2021).
[13] M. Block, D. Ackermann, K. Blaum, C. Droese, M. Dworschak, S. Eliseev, T. Fleckenstein, E. Haettner, F. Herfurth, F. P. Heßberger, S. Hofmann, J. Ketelaer, J. Ketter, H.-J. Kluge, G. Marx, M. Mazzocco, Y. N. Novikov, W. R. Plaß, A. Popeko, S. Rahaman *et al.*, Nature (London) **463**, 785 (2010).
[14] M. A. Stoyer, Nature (London) **442**, 876 (2006).
[15] N. Rowley, Nature (London) **400**, 209 (1999).
[16] J. Jackson, Can. J. Phys. **34**, 767 (1956).
[17] M. Kowal, P. Jachimowicz, and A. Sobiczewski, Phys. Rev. C **82**, 014303 (2010).
[18] Z.-Q. Feng, G.-M. Jin, F. Fu, and J.-Q. Li, Nucl. Phys. A **771**, 50 (2006).
[19] G. G. Adamian, N. V. Antonenko, S. P. Ivanova, and W. Scheid, Phys. Rev. C **62**, 064303 (2000).
[20] M. Bender, R. Bernard, G. Bertsch, S. Chiba, J. Dobaczewski, N. Dubray, S. A. Giuliani, K. Hagino, D. Lacroix, Z. Li *et al.*, J. Phys. G: Nucl. Part. Phys. **47**, 113002 (2020).
[21] G. N. Smirenkin, IAEA Report No. INDC(CCP)-359 (1993), https://www-nds.iaea.org/RIPL-3/.
[22] P. Möller, A. J. Sierk, T. Ichikawa, A. Iwamoto, R. Bengtsson, H. Uhrenholt, and S. Åberg, Phys. Rev. C **79**, 064304 (2009).
[23] A. Mamdouh, J. Pearson, M. Rayet, and F. Tondeur, Nucl. Phys. A **644**, 389 (1998).
[24] A. Mamdouh, J. Pearson, M. Rayet, and F. Tondeur, Nucl. Phys. A **679**, 337 (2001).
[25] A. Dobrowolski, K. Pomorski, and J. Bartel, Phys. Rev. C **75**, 024613 (2007).
[26] K. Pomorski and J. Dudek, Phys. Rev. C **67**, 044316 (2003).
[27] S. E. Agbemava, A. V. Afanasjev, D. Ray, and P. Ring, Phys. Rev. C **95**, 054324 (2017).
[28] T. Bayram, S. Akkoyun, and S. O. Kara, J. Phys. Conf. Ser. **490**, 012105 (2014).
[29] S. Akkoyun, T. Bayram, and T. Turker, Radiat. Phys. Chem. **96**, 186 (2014).
[30] S. Athanassopoulos, E. Mavrommatis, K. Gernoth, and J. W. Clark, Nucl. Phys. A **743**, 222 (2004).
[31] T. Bayram, S. Akkoyun, and S. O. Kara, Ann. Nucl. Energy **63**, 172 (2014).
[32] H. F. Zhang, L. H. Wang, J. P. Yin, P. H. Chen, and H. F. Zhang, J. Phys. G: Nucl. Part. Phys. **44**, 045110 (2017).
[33] R.-D. Lasseri, D. Regnier, J.-P. Ebran, and A. Penon, Phys. Rev. Lett. **124**, 162502 (2020).
[34] D. Lay, E. Flynn, S. A. Giuliani, W. Nazarewicz, and L. Neufcourt, Phys. Rev. C **109**, 044305 (2024).
[35] X. Bao, H. Zhang, G. Royer, and J. Li, Nucl. Phys. A **906**, 1 (2013).
[36] V. I. Zagrebaev, Phys. Rev. C **67**, 061601(R) (2003).
[37] X. J. Bao, Y. Gao, J. Q. Li, and H. F. Zhang, Phys. Rev. C **92**, 034612 (2015).
[38] A. S. Zubov, G. G. Adamian, N. V. Antonenko, S. P. Ivanova, and W. Scheid, Phys. Rev. C **65**, 024308 (2002).
[39] E. Cherepanov, A. Iljinov, and M. Mebel, J. Phys. G **9**, 931 (1983).
[40] Z.-Q. Feng, G.-M. Jin, J.-Q. Li, and W. Scheid, Nucl. Phys. A **816**, 33 (2009).
[41] T. Bürvenich, M. Bender, J. A. Maruhn, and P.-G. Reinhard, Phys. Rev. C **69**, 014307 (2004).
[42] M. G. Itkis, Y. T. Oganessian, and V. I. Zagrebaev, Phys. Rev. C **65**, 044602 (2002).
[43] U. Forsberg, D. Rudolph, L.-L. Andersson, A. Di Nitto, C. E. Düllmann, C. Fahlander, J. Gates, P. Golubev, K. Gregorich, C. Gross *et al.*, Nucl. Phys. A **953**, 117 (2016).
[44] Y. T. Oganessian, V. K. Utyonkov, N. D. Kovrizhnykh, F. S. Abdullin, S. N. Dmitriev, D. Ibadullayev, M. G. Itkis, D. A. Kuznetsov, O. V. Petrushkin, A. V. Podshibiakin, A. N. Polyakov, A. G. Popeko, R. N. Sagaidak, L. Schlattauer, I. V. Shirokovski, V. D. Shubin, M. V. Shumeiko, D. I. Solovyev, Y. S. Tsyganov, A. A. Voinov *et al.*, Phys. Rev. C **106**, L031301 (2022).
[45] Y. T. Oganessian, V. K. Utyonkov, N. D. Kovrizhnykh, F. S. Abdullin, S. N. Dmitriev, A. A. Dzhioev, D. Ibadullayev, M. G. Itkis, A. V. Karpov, D. A. Kuznetsov, O. V. Petrushkin, A. V. Podshibiakin, A. N. Polyakov, A. G. Popeko, I. S. Rogov, R. N. Sagaidak, L. Schlattauer, V. D. Shubin, M. V. Shumeiko, D. I. Solovyev *et al.*, Phys. Rev. C **106**, 064306 (2022).
[46] Y. T. Oganessian, A. V. Yeremin, A. G. Popeko, S. L. Bogomolov, G. V. Buklanov, M. L. Chelnokov, V. I. Chepigin, B. N. Gikal, V. A. Gorshkov, G. G. Gulbekian, M. G. Itkis, A. P. Kabachenko, A. Y. Lavrentev, O. N. Malyshev, J. Rohac, R. N. Sagaidak, S. Hofmann, S. Saro, G. Giardina, and K. Morita, Nature (London) **400**, 242 (1999).